

Grid Interconnection of Renewable Energy Sources using Multifunctional Grid Interactive Inverters

N. Rajeshwari¹, A. Naveen Kumar²

¹PG Scholar, ²Professor, ^{1,2}Department of Electrical and Electronics Engineering

^{1,2}Anurag Group of Institutions, Hyderabad, Telangana, India

Email ID: rajeshwari5519@gmail.com, naveenkumareee@cvsr.ac.in

Abstract

This paper proposes a lively calculation of MFGIIs under unequalled weights and under the fundamental voltage conditions for Multifunctional Grid Tie inverters. For design of an MFGII controller, the proposed calculation uses rapid power speculation. An estimator for Positive Fundamental Components (PFCE) is used to monitor unwanted components of a pile current such as tone, reactive current and negative plan components. The PFCE is an open-circle lightweight calculation. Unbelievable goodness is then refined with the inconvenience of less machine. Furthermore, a sliding mode (SMC) controller is used to improve a special display and energy against the limit range as a transmission voltage controller. The MFGII interfaces with the microgrid to the critical grid at a common connection point (PCC). A proposed control computing enables the MFGII to redeem open resources, mitigate music and balance a pile in the vicinity of a unique power implantation. This paper provides an unmistakable sample evaluation of SAPF, explicitly under two current control philosophies, quick dynamical and sensitive power speculations (p-q) and composite border comparison theory (d-q). The reference current for a channel is generated in two procedures, compensating either for open power or a constant current part in a power structure.

Keywords:renewable energy source, grid interconnection, current regulator, DC regulator.

1. Introduction

Over a period of two or three years, an energy system has moved to a Distributed Generation (DG) with Renewable Energy Sources[1] from a central era subject to oil-based products. The social affair of such DG units and weights in the microgrid lies under a new sharp grid thinking. A microgrid consists of the total DG units and neighbourhood loads and appears as a bidirectional dynamic load together as a rule grid[2]. The microgrid can absorb or transfer powerful grid capacity as a partner with a grid. Because of the grid defect, the microgrid should have an option to function in the island fashion. A microgrid is connected to a grid by a single point, a common connection point (PCC). In order to be linked to a key grid, the microgrid must meet the basic power quality constraints of an IEEE 519-2014[3] and IEEE 1547[4] power system operator among these. Most DG units use grid interfaces with power contraptions [5]. These converters can be used for various purposes through the improvement and their control estimates. In 2000[6] manufacturers analysed the usual use of a DG in order to provide subordinate assistance. This probability was used by the researchers to redesign a power concept of the microgrid via the multi-functional grid interactive (MFGII) inverter interface on a PCC[7]. In the immediate vicinity of a specific power supply from the DG, an MFGII can provide a microgrid with subordinate organisations such as consonant assistance, power factor cures and weight shift. The lot filed in the composing is a three-stage MFGII [8]. The SRF-PLL is widely used for the synchronisation of the MFGII to a grid and for music scans[8]. Using PLL meets the issue of grid repeat drift, non-ideal critical voltage assessment botch, and complicated estimates as inspected[26]. It is suggested to estimate the PLL-less power in [14]. No matter how grid repeat glides and delays problems are blocked, a stunning estimate problem persists. In addition, poor

isolation of the Total Harmonic Distortions (THD), most of which are high, can be observed. Unbalance is the great problem of power quality in close proximity to music. It affects the power and electrical equipment in conflict with each other. In addition to weakness and power problems on the impact system, the imbalance causes electric machine overheating, transformer turmoil and impact converter performance. A MFGII is used to change loads as subordinated organisations. The unbalance problem is tended to be addressed in [10]. In [14], a plan mix is used to envelop the structure of a device. In order to repay an imbalance, three-stage four-leg inverter is used in[10]. An additional leg appears to have an extra cost which is characterised by a simple 3-stage plan.

In [17] a three-stage action course is used. Despite the way that manufacturers have used the basic game plan, control calculations are rare. An incredible computation, a complicated inverter development or low performance represent a recent referred scheme for MFGII regulating and offering subordinate types of assistance. This paper uses the three-stage 3-wire inverter with simple and enthusiastic control calculations which ensure outstanding results with low estimates. This article examines a problem of control of MFGII in a deeply irritated atmosphere. Another Positive Fundamental Component Estimator PFCE, which is subject to sliding mode theory, is the main responsibility of this paper near another DC transport controller. The Sliding Mode Controller (SMC) combines the unbelievable presence and goodness with a range of device limits. A PFCE relies on the transformation chip away of the Adaptive Signal Generator Adaptable Quadrature (AQSG 3ph) in [27]. This epic kind of performance ensures a complex power imbue ment, sound payment, response power and a load change under dramatic basic voltage conditions. Three phases of an MFGII are regulated. A reference current for updating the power quality measurements an important step. In this case, a DC transport is detected as to what a specific power is to be injected if a RES pith event should develop or whether a RES non-attendance is to ingest a powerful power from the grid. Finally, an MFGII output current is regulated in a third step.

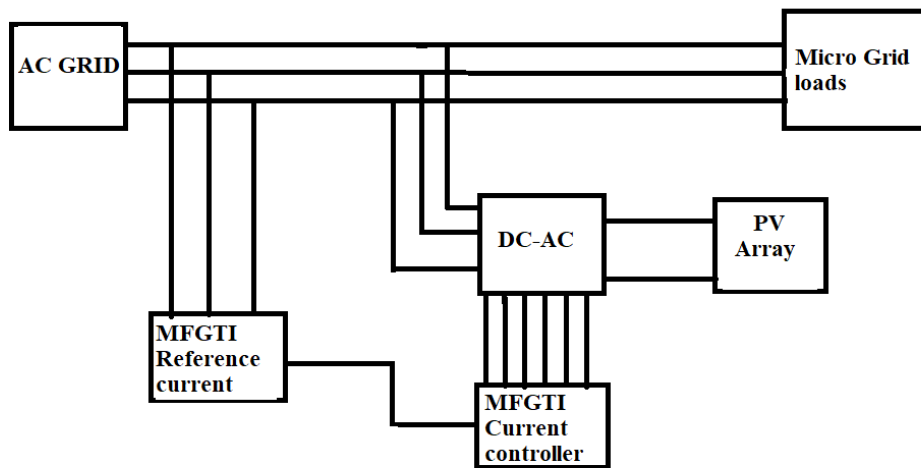


Fig. 1: System configuration.

2. System configuration

The common path of the microgrid related to a standard grid is shown in Fig. 1. The grid interface of the MFGII is related to the PCC. With a PCC link, MFGII really needs dynamic power injecting, music and sensitive power compensating and microgrid load balancing. Therefore, a microgrid is the directly modified, strong weight for a regular grid. The ability to alter a microgrid stream under unequal rules violation represents an additional advantage of an MFGII.

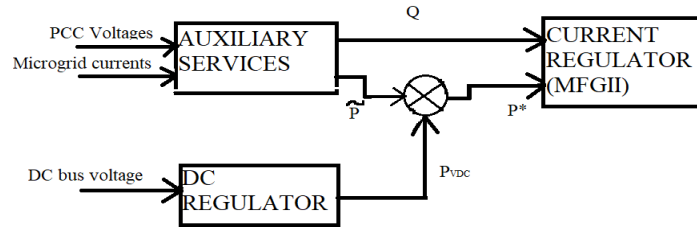


Fig. 2: Proposed MFGII control algorithm.

The submissions of MFGII rely essentially on a control estimate. A solid and rapid control computation is essential for rapid changes in a microgrid, basic grid aggravations and a sporadic RES definition. A point of this paper would subsequently be to prevent strategies subject to the facilitated diagram or to machine limits (PI based regulators).

3. Control algorithm

Another control method for the MFGII is proposed in this paper. Three phases of control occur (Fig. 2). In all cases, aid agencies are granted (symphonises balance, responsive power compensation, load changing, etc) At this stage, the mixing of a specific power provided with a RES restricts DC transport. In conclusion, an MFGII output current is monitored. Each show is dependent on an MFGII and large displays. Three estimates that unite simplicity, robustness and low computing requirements are subsequently used in this paper. A PFCE is used to provide a kind of assistance in the first level. The effect is to regulate a DC transport voltage and inject a single power by using an SMC controller. In a third, the new controller for hysteresis is used to improve its simplicity and robustness.

3.1 Background of an instantaneous power theory

In 1983, Akagi et al. suggested in either case pq speculation, a rapid power theory. This speculation records a fast power flowing through the 3-stage structure. It uses a Clarke flux and voltages change given by:

$$\begin{bmatrix} V_{alpha} \\ V_{beta} \end{bmatrix} = \sqrt{\frac{2}{3}} \begin{bmatrix} 1 & -\frac{1}{2} & -\frac{1}{2} \\ 0 & \frac{\sqrt{3}}{2} & -\frac{\sqrt{3}}{2} \end{bmatrix} \begin{bmatrix} V_a \\ V_b \\ V_c \end{bmatrix} \tag{1}$$

$$\begin{bmatrix} I_{alpha} \\ I_{beta} \end{bmatrix} = \sqrt{\frac{2}{3}} \begin{bmatrix} 1 & -\frac{1}{2} & -\frac{1}{2} \\ 0 & \frac{\sqrt{3}}{2} & -\frac{\sqrt{3}}{2} \end{bmatrix} \begin{bmatrix} I_a \\ I_b \\ I_c \end{bmatrix} \tag{2}$$

The instantaneous complex power is calculated:

$$S = e \cdot i^* = V_{alpha} I_{alpha} + V_{beta} I_{beta} + j(V_{beta} I_{alpha} - V_{alpha} I_{beta}) \tag{3}$$

Two new substances are depicted in this way, a short true power *p* and a quick non-existent power *q* where:

$$P = V_{alpha} I_{alpha} + V_{beta} I_{beta} = \bar{P} + \tilde{P} \tag{4}$$

$$Q = V_{beta} I_{alpha} + V_{alpha} I_{beta} = \bar{Q} + \tilde{Q} \tag{5}$$

The sparkling speculation in power is charming for the sensitive and routine value of a new three-stage method. In (4) a true power *p* leads to a solitary way of streaming energy per time unit (from a

source to a load and a opposite way around). An active power (p) addresses the energy transferred, per unit of time. The winding section of the whole thing thinks of an energy exchanged from a source to a stack per unit of time. An active power of the system definition, null, never less than the proportion of power that flows every time. It's a beginning of the deplorable current from this point on. A whimsical power q is depicted as an exchange of energy between three-step structural wires. At each stage the power spilled and identified with a whimsical power therefore does not add to an energy movement at any point of the second between a source and a load. These attestations can be collected from an above explanation: Two components will break down a certified power p . The coherent fast component p tends towards a strong force, and the twisted part of it tends towards the tone. Moreover, the non-existent power is declined to the immediate piece q which suggests an accessible power and a portion that influences sounds sensitive. As words, alternative to alternative, alternative, q does not contribute to the movement from a source to a stack. As required, they can be reimbursed without fuel sources using the three-stage inverter. This technique advances in determining a music in a time territory. Different experts have suggested that this technique be improved and changed for efficient filtering. A diagram of power in the microgrid in seeing the MFGII is depicted in Fig.3. The certifiable quick power p can draw loads in a microgrid. In the light of the non-linear concept of stacks this true power involves the working power and the twisting energy. The transitory whimsical power q shall be shared between microgrid periods.

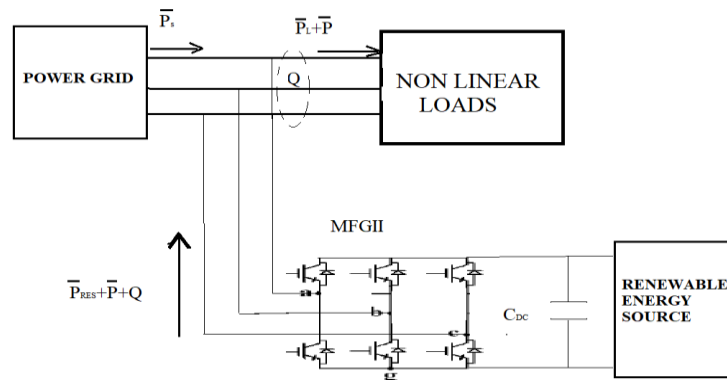


Fig. 3. Illustration of instantaneous power theory in the microgrid.

A MFGII is used to provide a specific RES (pRES) power mixing system to improve a power idea of a microgrid and allow a grid to provide the only power provided by a microgrid in that it provides:

$$\bar{P}_L = \bar{P}_S + \bar{P}_{RES} \tag{6}$$

As a result, a microgrid is basically resistive from a microgrid perspective . Compensation of \bar{sop} and q would enhance the micro grid power concept that gives money and environmental advantages [14]. In order to disconnect words, the manufacturers propose to use the low or high pass filter (LPF or HPF). This leads to delay and inaccuracy in any situation. This paper suggests a use of the PFCE to crush this cut-off. A brief description of power speculation will be used to evaluate the multifunctional grid inverter benchmark. Maybe a key component of voltages and streams is taken from the filtering of a true and whimsical force suggested by a primary method. A flat part of a stream (music) is resolved by then. By then. From here a power is resolved by means of quick definitions of power speculation. Using the proposed PFCE, a fundamental portion is mined. An significant drawback of pq theory is prevented by preventing the use of LPF or HPF. The accurate extraction under injury or imbalance guideline voltage will be enabled by the use of the PFCE.

3.2 The positive fundamental component estimator

The modified interpretation of a 3ph-AQSG, introduced, is used to eliminate an important positive collection of a microgrid stream. A constructive game plan for an information signal under a fixed

repeat will be evaluated by PFCE provided in Fig. 4. A synchronous grid voltage difference is indicated

$$V_{dq} = \begin{bmatrix} v_d \\ v_q \end{bmatrix} = \frac{2}{3} \begin{bmatrix} \cos(\omega_0 t) & \cos(\omega_0 t - \frac{2\pi}{3}) & \cos(\omega_0 t - \frac{4\pi}{3}) \\ \sin(\omega_0 t) & \sin(\omega_0 t - \frac{2\pi}{3}) & \sin(\omega_0 t - \frac{4\pi}{3}) \end{bmatrix} \begin{bmatrix} v_a \\ v_b \\ v_c \end{bmatrix} \quad (7)$$

Due to the voltage imbalance, the positive and negative progression of two components v_d and v_q could be reduced:

$$V_{dq} = V^p_{dq} + V^n_{dq} \quad (8)$$

The novel model of this estimator should be developed in order to create a PFCE. From a synchronous reference diagram element, a fixed fragment can be obtained through a ω modification:

$$V_{alphanumeric} = V^p_{alphanumeric} + V^n_{alphanumeric} = e^{j\omega_0 t} V^p_{dq} + e^{-j\omega_0 t} V^n_{dq} \quad (9)$$

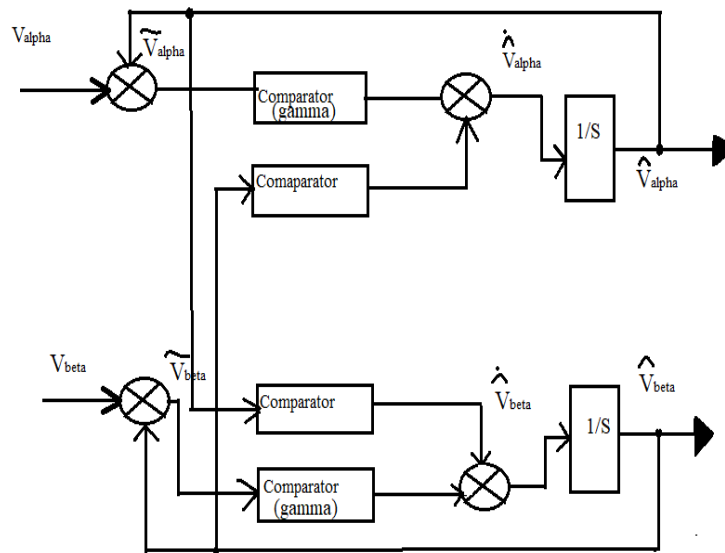


Fig. 4: Positive fundamental components estimator.

Were

$$e^{j\omega_0 t} = \begin{bmatrix} \cos\omega_0 t & \sin\omega_0 t \\ -\sin\omega_0 t & \cos\omega_0 t \end{bmatrix}, J = \begin{bmatrix} 0 & -1 \\ 1 & 0 \end{bmatrix}$$

The imitative of a $\alpha\beta$ is shown by:

$$\dot{v}_{alphanumeric} = \omega_0 J (v^p_{alphanumeric} - v^n_{alphanumeric}) \quad (10)$$

The proposed estimator incorporates a saturated term applied to the model structure (9):

$$\hat{v}_{alphanumeric} = \omega_0 J (v^p_{alphanumeric} - v^n_{alphanumeric}) + \lambda \tilde{v}_{alphanumeric} \quad (11)$$

v_α upstream: Basic tension, $\hat{v} \sim v$ $\alpha\beta$, down downstream from damping factor λ . It is important that a PFCE can be used on voltage fundamental $\alpha\beta$:

3.3 PFCE differentiation of different methods

- In a fixed reference graph, a PFCE is performed. No mathematical evaluation is essential.

- Calculations essential, increments and duplications easy. There are no unbelievable estimates.
- A PFCE is a lightweight speed calculation that simplifies the operation of the simple processor taking into account more than two points.
- A PFCE is an unambiguously consistent approach for the open circle. A bode-graph of a PFCE in Fig.6 insists this argument. A PFCE is consistently compatible with a last referenced one.
- In a data signal at a grid repeat no lag is added as shown in Fig.6.
- A PFCE would correctly evaluate the fundamentally positive portion of a grid replay, instead of an LPF (Fig.6). Normally, an estimate would be prepared to reimburse a negative voltage or weight unbalance set.

3.4. Reference power calculation

The streams in hatchets $\alpha\beta$ can be separately rotted into dc and ac components:

$$I_{\alpha} = \hat{I}_{\alpha} + \tilde{I}_{\alpha} \tag{12}$$

$$I_{\beta} = \hat{I}_{\beta} + \tilde{I}_{\beta} \tag{13}$$

The above-analysed PFCE removes a fundamental component at a pulsate ω_0 directly from a streams in hatchets $\alpha\beta$ (Fig. 4). Starting there ahead, a consonant components of a pile streams are enlisted by removing fundamental components from a microgrid current (Fig. 6).

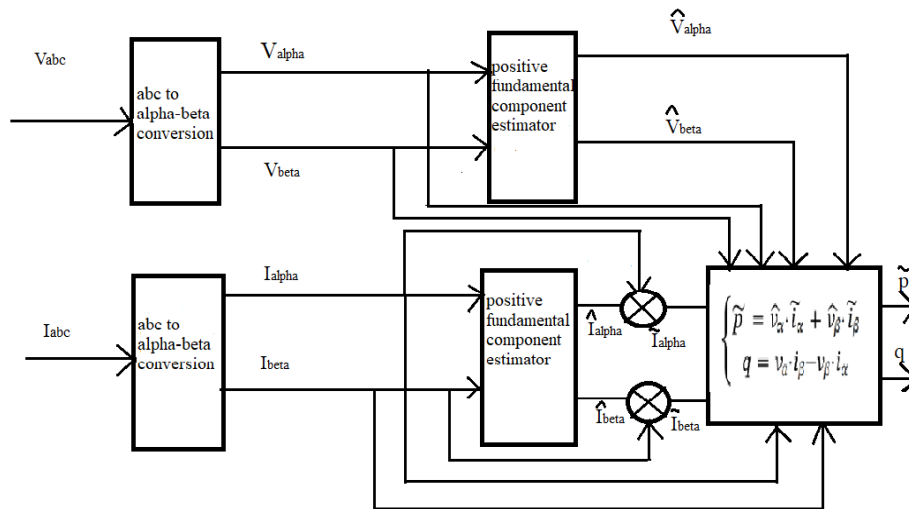


Fig. 6: PFCE based \tilde{p} and \tilde{q} estimator.

$$\tilde{I}_{\alpha} = I_{\alpha} - \hat{I}_{\alpha} \tag{14}$$

$$\tilde{I}_{\beta} = I_{\beta} - \hat{I}_{\beta} \tag{15}$$

Certifiable and whimsical powers are then decided as portrayed in a transient power speculation [36]:

$$\tilde{P} = \hat{V}_{\alpha} \cdot \tilde{I}_{\alpha} + \hat{V}_{\beta} \cdot \tilde{I}_{\beta} \tag{16}$$

$$q = V_{\alpha} \cdot I_{\beta} - V_{\beta} \cdot I_{\alpha} \tag{17}$$

The controller of DC transport DC dynamic transport presentations are of the utmost importance for the MFGII work. An extraordinary idea of a microgrid makes it imperative that a regulator be inhuman to device limitations, essential voltage, and weight. Naturally, a response time should be very fast in order to arrange for rapid adjustments to the RES and grid differences. This paper therefore recommends a sliding mode solution, as opposed to the PI regulator used in [8], which has

proved extremely difficult in these circumstances to adjust. A strong SMC and a rapid response time is established. A square slider controller chart made to monitor a Vdc is shown in Fig. 7. Fig. 7. Due to the strength and rapid reaction time, an SMC is considered to be ludicrous. The performance of the controller is a unique ability. In Section 3.3, this influence is applied to the influencing power. In any case, a state variable x1 is represented as a botch between Vdc and the reference:

$$x_1 = v_{dc}^* - v_{dc} \tag{18}$$

The second state variable x2 is described as an auxiliary of x1

$$x_2 = \dot{x}_1 \tag{19}$$

The value of a trading limits y1 and y2 are described as follows [38]:

$$\begin{aligned} y_1 &= 1 && \text{if } z\kappa_1 > 0 \\ y_1 &= -1 && \text{if } z\kappa_1 < 0 \\ y_2 &= 1 && \text{if } z\kappa_2 > 0 \\ y_2 &= -1 && \text{if } z\kappa_2 < 0 \end{aligned}$$

where z is a trading limit $z\kappa = +112$. c1 and c2 are positive reliable. a yield of a sliding mode controller Un is taken as:

$$U_n = \kappa_1 y_1 + \kappa_2 y_2 \tag{21}$$

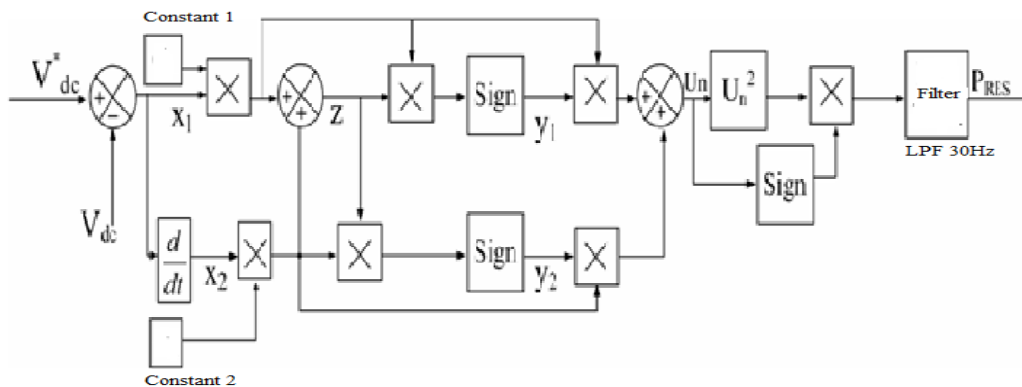


Fig. 7: SMC block diagram.

This is the strong strength of PRES: $PRES = U \text{ sign}(U_n)^2$ (18) $\text{sign}(U_n)$ word handles cases where there is a RES incidence deficit. The low-pass channel with a 30 Hz repeat is added to limit movements in a return capacity.

4. Control block diagram

A diagram of Fig. 8 describes the complete supervision estimate. A reference current in the reference diagram of the $\alpha\beta$ is dictated by the addition of an adjustable dynamic power necessary to regulate a transportation DC (PRES) voltage in an elective part of a speedy actual power determined in (13).

$$i_{\alpha}^* = \frac{\hat{v}_{\alpha}}{\hat{v}_{\alpha}^2 + \hat{v}_{\beta}^2} (\tilde{P} + P_{RES}) - \frac{\hat{v}_{\beta}}{\hat{v}_{\alpha}^2 + \hat{v}_{\beta}^2} q \tag{22}$$

$$i_{\beta}^* = \frac{\hat{v}_{\beta}}{\hat{v}_{\alpha}^2 + \hat{v}_{\beta}^2} (\tilde{P} + P_{RES}) - \frac{\hat{v}_{\alpha}}{\hat{v}_{\alpha}^2 + \hat{v}_{\beta}^2} q \tag{23}$$

Current references have two fuse words from (19). The basic term contains a consonant current portion and the resulting consonant consists of a basic current fragment at store voltage level. Thus, the proportion of dynamic capacity is consumed by a dc transport voltage from or transferred to a dc

condenser; likewise reactive streams are developed for maintaining microgrid streams in the supply voltage level. By that time, a diversion of references will be seen in a–b–c headings by:

$$\begin{bmatrix} i_{fa}^* \\ i_{fb}^* \\ i_{fc}^* \end{bmatrix} = \sqrt{\frac{2}{3}} \begin{bmatrix} 1 & 0 \\ \frac{1}{2} & \frac{\sqrt{3}}{2} \\ -\frac{1}{2} & -\frac{\sqrt{3}}{2} \end{bmatrix} \begin{bmatrix} i_{\alpha}^* \\ i_{\beta}^* \end{bmatrix} \quad (24)$$

The reference current received from (20) is transferred to a current controller. Due to its simplicity and robustness the hysteresis-based current controller is used in this article.

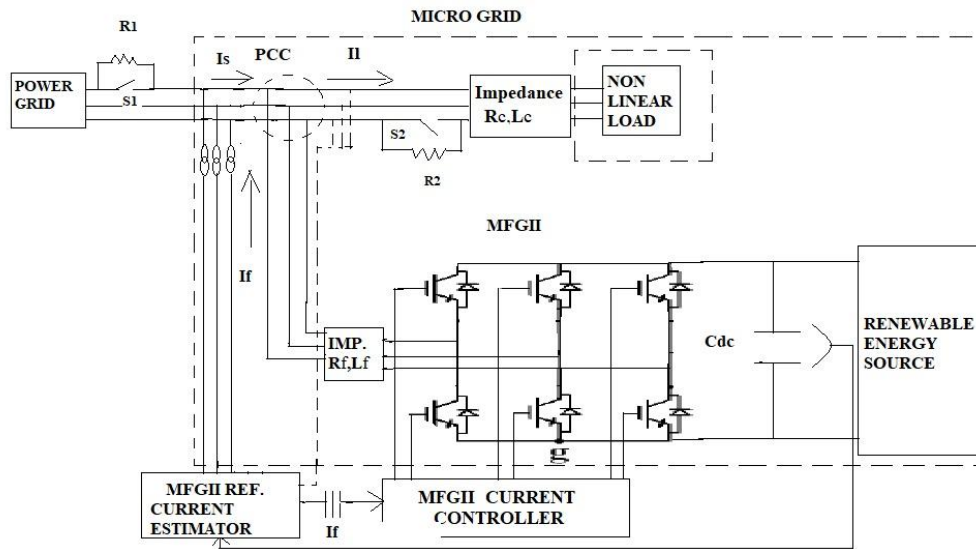


Fig. 9: Schematic of a tested system.

4.1 P-Q method Mathematical modelling

A transition from Clarke, which can be seen by a gear with conditions 1 and 2, is the connection between charge current and voltage of the three phase power system and an equal heading structure (α - β -0).

$$\begin{bmatrix} V_{\alpha} \\ V_{\beta} \end{bmatrix} = \sqrt{\frac{2}{3}} \begin{bmatrix} 1 & -\frac{1}{2} & -\frac{1}{2} \\ 0 & \frac{\sqrt{3}}{2} & -\frac{\sqrt{3}}{2} \end{bmatrix} \begin{bmatrix} V_a \\ V_b \\ V_c \end{bmatrix} \quad (25)$$

$$\begin{bmatrix} I_{\alpha} \\ I_{\beta} \end{bmatrix} = \sqrt{\frac{2}{3}} \begin{bmatrix} 1 & -\frac{1}{2} & -\frac{1}{2} \\ 0 & \frac{\sqrt{3}}{2} & -\frac{\sqrt{3}}{2} \end{bmatrix} \begin{bmatrix} I_a \\ I_b \\ I_c \end{bmatrix} \quad (26)$$

Short power can be found even in the coordinate system by copying a transient current with a quick voltage view. Here, a 3-phase structure is usually balanced, so as condition 3 we can find brief control.

$$P = v_a i_a + v_b i_b + v_c i_c \quad (27)$$

A flat dynamic and open power can be modified from above in power system design as

$$\begin{bmatrix} p \\ q \end{bmatrix} = \begin{bmatrix} V_{\alpha} & V_{\beta} \\ -V_{\beta} & V_{\alpha} \end{bmatrix} \begin{bmatrix} I_{\alpha} \\ I_{\beta} \end{bmatrix} \quad (28)$$

The fast reaction force causes the negative vector to drop a consonant part in a line current at a 180-degree level. From a foregoing state, yield 5

$$\begin{bmatrix} i^*_{\text{salpha}} \\ i^*_{\text{sbeta}} \end{bmatrix} = \frac{1}{v_{\text{alpha}}^2 + v_{\text{beta}}^2} \begin{bmatrix} V_{\text{alpha}} & -V_{\text{beta}} \\ V_{\text{beta}} & V_{\text{alpha}} \end{bmatrix} [P_0 + P_{\text{loss}}] \quad (29)$$

A compensating current for any phase can be determined by using an opposite shift of Clarke, as illustrated in condition 6 to find an α - β reference current.

$$\begin{bmatrix} i^*_{\text{ca}} \\ i^*_{\text{cb}} \\ i^*_{\text{ca}} \end{bmatrix} = \sqrt{\frac{2}{3}} \begin{bmatrix} 1 & 0 \\ -\frac{1}{2} & \frac{\sqrt{3}}{2} \\ -\frac{1}{2} & -\frac{\sqrt{3}}{2} \end{bmatrix} \begin{bmatrix} i_{\text{s alpha}} \\ i_{\text{s beta}} \end{bmatrix} \quad (30)$$

4.2 D-Q method Mathematical modelling

The transition of Park's linkage to a d-q reference coordinate current is seen in condition 7 between 3-b-c current and a d-q coordinate current

$$\begin{bmatrix} i_{ld} \\ i_{lq} \\ i_{l0} \end{bmatrix} = \sqrt{\frac{2}{3}} \begin{bmatrix} \cos \mu & \cos \left(\mu - \frac{2\pi}{3} \right) & \cos \left(\mu + \frac{2\pi}{3} \right) \\ -\sin \mu & -\sin \left(\mu - \frac{2\pi}{3} \right) & -\sin \left(\mu + \frac{2\pi}{3} \right) \\ \frac{1}{\sqrt{2}} & \frac{1}{\sqrt{2}} & \frac{1}{\sqrt{2}} \end{bmatrix} \begin{bmatrix} i_{la} \\ i_{lb} \\ i_{lc} \end{bmatrix} \quad (31)$$

Where " μ " is an exact difference of a planned 3-stage balanced device reference diagram which is the right limit of the basic repeat. A reference current of symphonis can be obtained from clear LPF load streams. A stream can be decayed into two components under Condition 8 and 9 in a concurrent reference structure.

$$i_{ld} = i^-_{ld} + i^{\sim}_{ld} \quad (32)$$

$$i_{lq} = i^-_{lq} + i^{\sim}_{lq} \quad (33)$$

Following isolation of DC terms, the terms trading appear in an extraction scheme in a yield that is likely to impair symphonics in the power structure. Condition 10 provides for APF comparison streams

$$\begin{bmatrix} i^*_{fd} \\ i^*_{fq} \end{bmatrix} = \begin{bmatrix} i^{\sim}_{ld} \\ i^{\sim}_{lq} \end{bmatrix} \quad (34)$$

A retrograde park shift, as shown in condition 11, is used to find a diversion stream in three phase structures which drops a consonant part in line side.

$$\begin{bmatrix} i^*_{fa} \\ i^*_{fb} \\ i^*_{fc} \end{bmatrix} = \sqrt{\frac{2}{3}} \begin{bmatrix} \cos \mu & -\sin \mu \\ \cos \left(\mu - \frac{2\pi}{3} \right) & -\sin \left(\mu - \frac{2\pi}{3} \right) \\ \cos \left(\mu + \frac{2\pi}{3} \right) & \sin \left(\mu + \frac{2\pi}{3} \right) \end{bmatrix} \begin{bmatrix} i^*_{fd} \\ i^*_{fq} \end{bmatrix} \quad (35)$$

5. Results

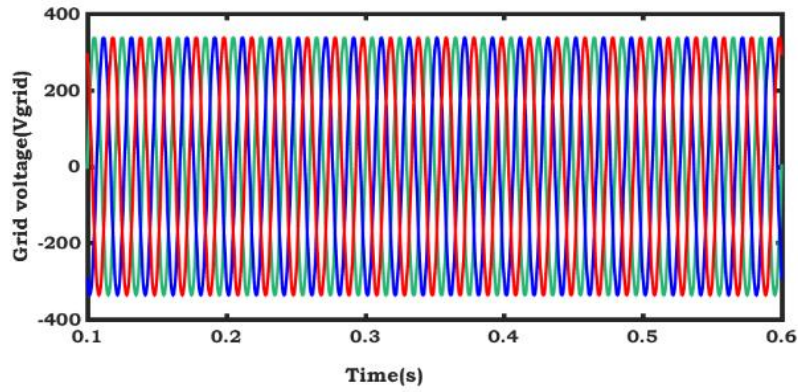


Fig. 10: Grid voltages.

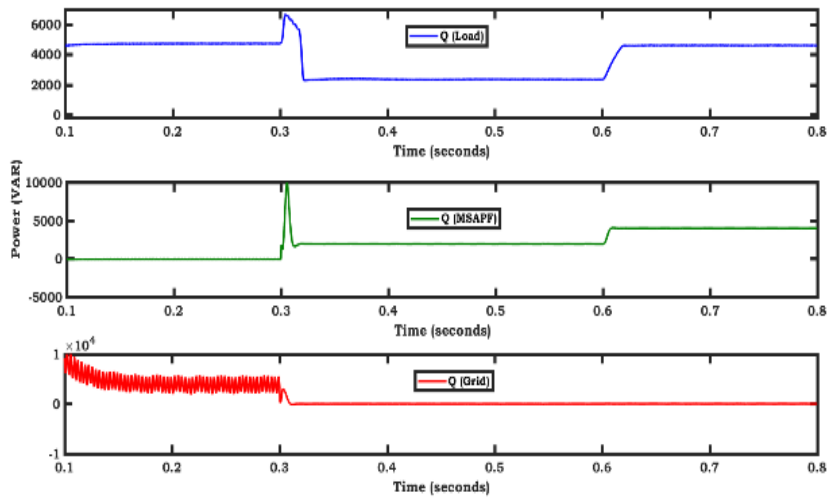


Fig. 11: A reactive powers of load MSAPF and Grid at $t=0.3$ to 0.6 in a load and MSAPF deviations are occurred but in grid there no deviations.

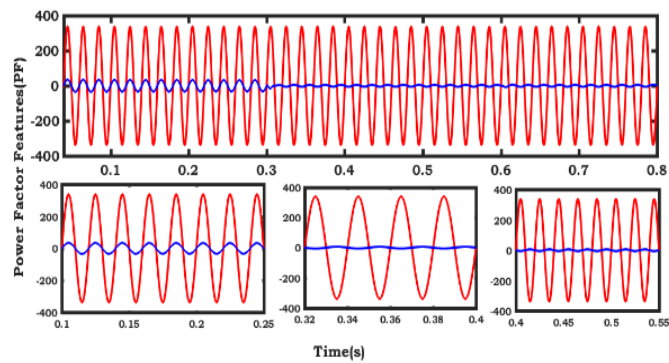


Fig. 12: Power factor correction of a grid at a time period 0.3 currents are suppressed to nearly 0.

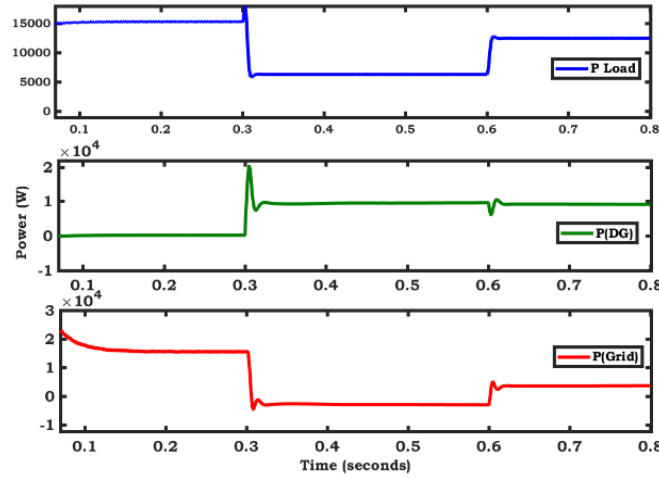


Fig. 13:Active power of a load, MSAPF and grid at a time period $t=0.3$ to 0.6 , load from 15kW to 5kW, DG from 0 to 20kW and grid powers from 2kW to 0.

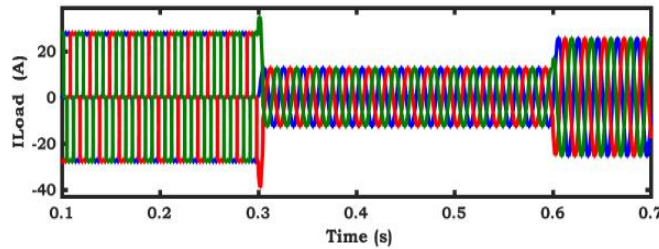


Fig. 14: Load currents has the sag from time $t=0.3$ to 0.6 from 22A to 10A and at $t=0.6$ 20A

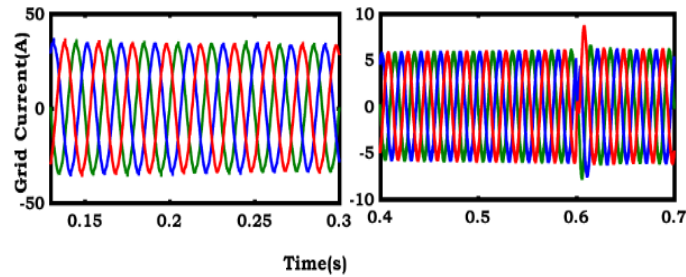


Fig. 15: Grid currents at $t=0.6$ the slight deviation is occurred and settled.

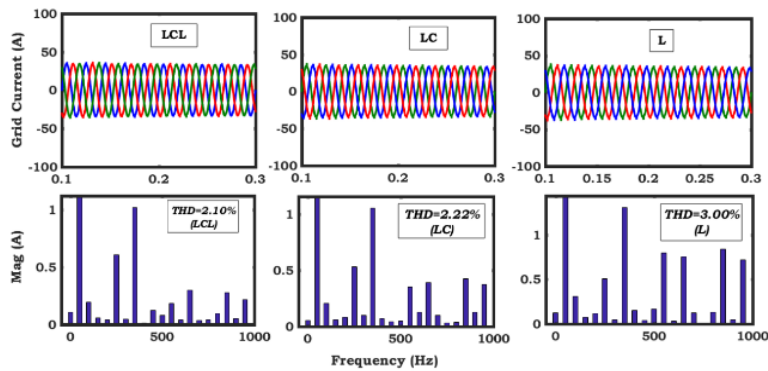


Fig. 16: Grid currents with LCL, LC and L with THDs of 2.10%, 2.22% and 3.00%.

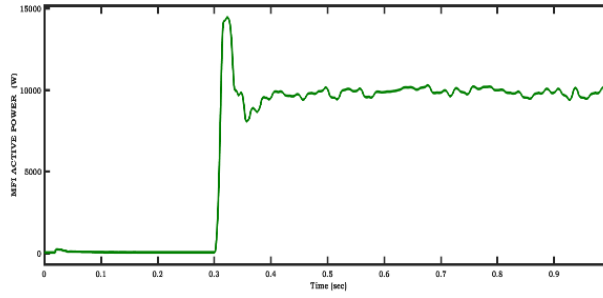


Fig. 17: MFGII active power

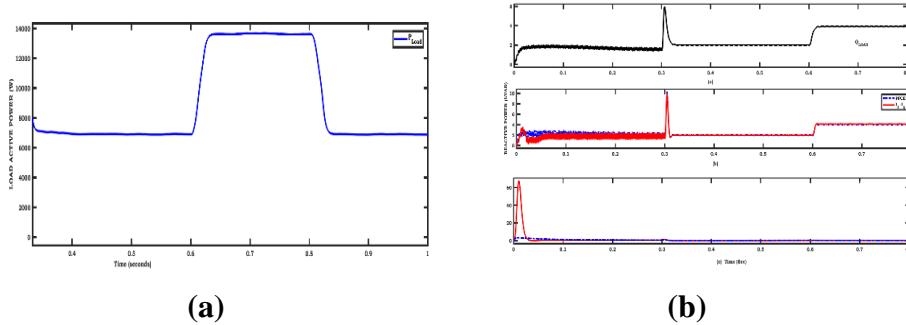


Fig. 18:(a) load active power. (b) reactive power

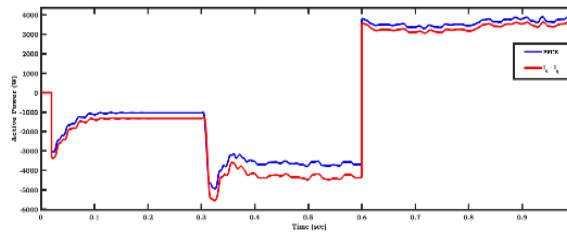


Fig. 19: Active power

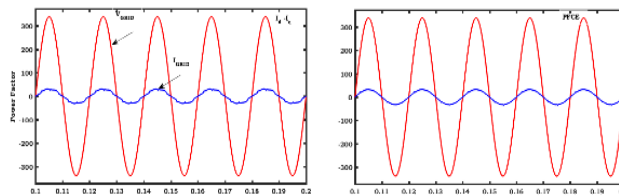


Fig. 21: Power factor

6. Conclusion

The microgrid should meet the power quality requirements in order to be combined with a fundamental grid. The MFGII is a convincing response from an inexhaustible source to infuse dynamic force and offers auxiliary aid types to help improve a micro grid's power. However, MFGII displays are affected by a primary voltage bother and a microgrid. In this paper, it is suggested that the MFGII be powerfully regulated in unbalanced conditions. The MFGII is used to infuse RES-based dynamic power, compensate for reactive forces and sounds, and balance the flow of a microgrid. In three steps, the initiated calculation is carried out. The PFCE-SMC mix is a lightweight and efficient arrangement that provides great displays under unfortunate main voltage and burden conditions. The exploratory results show the feasibility and improvement of the force existence of a

microgrid by a proposed PFCE-SMC measurement. Considering that by using d-q control methodology, the consonant will be compensated favourably instead of p-q, for example, a THD of source stream will almost dramatically decrease while using a d-q technique. Since the door card is not available to the driver, we cannot complete a test arrangement and endorse the result of the recast. To ensure the reliability and security of a framework by means of the current regulatory system based on PWM, the preferred route can be tracked in future over d-q to wipe out sonographic sound within the efficiency of the power system.

REFERENCES

- [1] Strasser T, et al. A review of architectures and concepts for intelligence in future electric energy systems. *IEEE Trans Ind Electron* Apr. 2015;62(4):2424–38.
- [2] Lasseter RH. MicroGrids. *IEEE power engineering society winter meeting*, vol. 1. 2002. p. 305–8.
- [3] IEEE Recommended Practice and Requirements for Harmonic Control in Electric Power Systems. In: *IEEE Std 519–2014 Revis. IEEE Std 519–1992*; Jun. 2014. p. 1–29
- [4] IEEE Application Guide for IEEE Std 1547(TM), IEEE Standard for Interconnecting Distributed Resources with Electric Power Systems. In: *IEEE Std 15472–2008*; Apr. 2009. p. 1–217.
- [5] Zeng Z, Yang H, Zhao R, Cheng C. Topologies and control strategies of multifunctional grid-connected inverters for power quality enhancement: a comprehensive review. *Renew Sustain Energy Rev* 2013;24:223–70.
- [6] Joos G, Ooi BT, McGillis D, Galiana FD, Marceau R. The potential of distributed generation to provide ancillary services. *IEEE power engineering society summer meeting*, vol. 3. 2000. p. 1762–7.
- [7] Miveh MR, Rahmat MF, Ghadimi AA, Mustafa MW. Power quality improvement in autonomous microgrids using multi-functional voltage source inverters: a comprehensive review. *J Power Electron* 2015;15(4):1054–65.
- [8] Poursmaeil E, Miguel-Espinar C, Massot-Campos M, Montesinos-Miracle D, GomisBellmunt O. A control technique for integration of DG units to the electrical networks. *IEEE Trans Ind Electron* 2013;60(7):2881–93.
- [9] Tummuru NR, Mishra MK, Srinivas S. Multifunctional VSC controlled microgrid using instantaneous symmetrical components theory. *IEEE Trans Sustain Energy* 2014;5(1):313–22.
- [10] Li Y, Vilathgamuwa DM, Loh PC. Microgrid power quality enhancement using a three-phase four-wire grid-interfacing compensator. *IEEE Trans Ind Appl* 2005;41(6):1707–19.
- [11] Zou Z, Wang Z, Cheng M. Modeling, analysis, and design of multifunction gridinterfaced inverters with output LCL filter. *IEEE Trans Power Electron* 2014;29(7):3830–9.
- [12] Acuna P, Moran L, Rivera M, Dixon J, Rodriguez J. Improved active power filter performance for renewable power generation systems. *IEEE Trans Power Electron* 2014;29(2):687–94.
- [13] Singh M, Chandra A. Real-time implementation of ANFIS control for renewable interfacing inverter in 3P4W distribution network. *IEEE Trans Ind Electron* 2013;60(1):121–8.
- [14] Wang F, Duarte JL, Hendrix MAM. Grid-interfacing converter systems with enhanced voltage quality for microgrid application—concept and implementation. *IEEE Trans Power Electron* 2011;26(12):3501–13.

- [15] Li YW, Vilathgamuwa DM, Loh PC. A grid-interfacing power quality compensator for three-phase three-wire microgrid applications. *IEEE Trans Power Electron* Jul. 2006;21(4):1021–31.
- [16] Guerrero JM, Loh PC, Lee T-L, Chandorkar M. Advanced control architectures for intelligent microgrids—Part II: power quality, energy storage, and AC/DC microgrids. *IEEE Trans Ind Electron* Apr. 2013;60(4):1263–70.
- [17] Nejabatkhah F, Li YW, Wu B. Control strategies of three-phase distributed generation inverters for grid unbalanced voltage compensation. *IEEE Trans Power Electron* 2016;31(7):5228–41.
- [18] Zeng Z, Yang H, Tang S, Zhao R. Objective-oriented power quality compensation of multifunctional grid-tied inverters and its application in microgrids. *IEEE Trans Power Electron* 2015;30(3):1255–65.
- [19] Munir S, Li YW. Residential distribution system harmonic compensation using PV interfacing inverter. *IEEE Trans Smart Grid* 2013;4(2):816–27.
- [20] Ouchen S, Betka A, Abdeddaim S, Menadi A. Fuzzy-predictive direct power control implementation of a grid connected photovoltaic system, associated with an active power filter. *Energy Convers Manage* 2016;122(Aug.):515–25.
- [21] He J, Li YW, Blaabjerg F. Flexible microgrid power quality enhancement using adaptive hybrid voltage and current controller. *IEEE Trans Ind Electron* 2014;61(6):2784–94.
- [22] Mehrasa M, Pouresmaeil E, Mehrjerdi H, Jørgensen BN, Catalão JPS. Control technique for enhancing the stable operation of distributed generation units within a microgrid. *Energy Convers Manage* 2015;97(Suppl. C):362–73.
- [23] Mehrasa M, Pouresmaeil E, Jørgensen BN, Catalão JPS. A control plan for the stable operation of microgrids during grid-connected and islanded modes. *Electr Power Syst Res* 2015;129(Suppl. C):10–22.
- [24] Mehrasa M, Adabi ME, Pouresmaeil E, Adabi J. Passivity-based control technique for integration of DG resources into the power grid. *Int J Electr Power Energy Syst* 2014;58(Suppl. C):281–90.
- [25] Guerrero-Rodríguez NF, Herrero-de Lucas LC, de Pablo-Gómez S, Rey-Boué AB. Performance study of a synchronization algorithm for a 3-phase photovoltaic gridconnected system under harmonic distortions and unbalances. *Electr Power Syst Res* 2014;116:252–65.
- [26] Feola L, Langella R, Testa A. On the effects of unbalances, harmonics and interharmonics on PLL systems. *IEEE Trans Instrum Meas* 2013;62(9):2399–409.
- [27] Escobar G, Martinez-Montejano MF, Valdez AA, Martinez PR, Hernandez-Gomez M. Fixed-reference-frame phase-locked loop for grid synchronization under unbalanced operation. *IEEE Trans Ind Electron* 2011;58(5):1943–51.
- [28] Watanabe EH, Aredes M, Afonso JL, Pinto JG, Monteiro LFC, Akagi H. Instantaneous p-q power theory for control of compensators in micro-grids. *International school on nonsinusoidal currents and compensation (ISNCC) 2010*;2010:17–26.
- [29] He J, Li Y, Blaabjerg F. Flexible microgrid power quality enhancement using adaptive hybrid voltage and current controller; 2014.
- [30] von Jouanne A, Banerjee B. Assessment of voltage unbalance. *IEEE Trans Power Deliv* 2001;16(4):782–90.

- [31] Dasgupta S, Mohan SN, Sahoo SK, Panda SK. Lyapunov function-based current controller to control active and reactive power flow from a renewable energy source to a generalized three-phase microgrid system. *IEEE Trans Ind Electron* 2013;60(2):799–813.
- [32] Meersman B, Renders B, Degroote L, Vandoorn T, Vandeveld L. Three-phase inverter-connected DG-units and voltage unbalance. *Electr Power Syst Res* 2011;81(4):899–906.
- [33] Kim H-S, Kim J-S, Kim K-H. Power quality improvement for grid connected inverters under distorted and unbalanced grids. *J Power Electron* 2016;16(4):1578–86.
- [34] Chilipi R, Sayari NA, Hosani KA, Beig AR. Control scheme for grid-tied distributed generation inverter under unbalanced and distorted utility conditions with power quality ancillary services. *IET Renew Power Gener* 2016;10(2):140–9.
- [35] Soshinskaya M, Crijns-Graus WHJ, Guerrero JM, Vasquez JC. Microgrids: experiences, barriers and success factors. *Renew Sustain Energy Rev* 2014;40:659–72.
- [36] Akagi H, Kanazawa Y, Nabae A. Instantaneous reactive power compensators comprising switching devices without energy storage components. *IEEE Trans Ind Appl* 1984;IA-20(3):625–30.
- [37] Akagi H, Watanabe EH, Aredes M. Instantaneous power theory and applications to power conditioning. 1st ed. Wiley-IEEE Press; 2007.
- [38] Asiminoaei L, Blaabjerg F, Hansen S. Detection is key – harmonic detection methods for active power filter applications. *IEEE Ind Appl Mag* 2007;13(4):22–33.
- [39] Green TC, Marks JH. Control techniques for active power filters. *Electr Power Appl IEE Proc* 2005;152(2):369–81.
- [40] Watanabe EH, Aredes M, Afonso JL, Pinto JG, Monteiro LFC, Akagi H. Instantaneous p–q power theory for control of compensators in micro-grids. In: 2010 international school on non-sinusoidal currents and compensation (ISNCC); 2010. p. 17–26.